Light Fan Driven by a Relativistic Laser Pulse

Yin Shi, Baifei Shen,* Lingang Zhang, Xiaomei Zhang, Wenpeng Wang, and Zhizhan Xu
State Key Laboratory of High Field Laser Physics, Shanghai Institute of Optics and Fine Mechanics, Chinese Academy of Sciences, Shanghai 201800, China
(Received 8 April 2014; published 10 June 2014)

When a relativistic laser pulse with a high photon density interacts with a specially tailored thin foil target, a strong torque is exerted on the resulting spiral-shaped foil plasma, or "light fan." Because of its structure, the latter can gain significant orbital angular momentum (OAM), and the opposite OAM is imparted to the reflected light, creating a twisted relativistic light pulse. Such an interaction scenario is demonstrated by particle-in-cell simulation as well as analytical modeling, and should be easily verifiable in the laboratory. As an important characteristic, the twisted relativistic light pulse has a strong torque and ultrahigh OAM density.

DOI: 10.1103/PhysRevLett.112.235001 PACS numbers: 52.38.-r, 03.50.De, 42.50.Tx, 52.59.-f

Prompted by the fast development of laser techniques [1], light-matter interaction has entered the regime of a relativistic laser-plasma interaction. Over the past few decades, a number of novel mechanisms and schemes have been proposed. Among these mechanisms and schemes, the most promising application is for use in laser-driven plasma accelerator science, such as laser wakefield acceleration of electrons [2] and a laser driving foil to accelerate protons [3]. Laser-plasma interaction can also be an efficient source of high-order harmonic generation (HHG) [4], x rays [5], and even gamma rays [6,7]. One of the key issues in the above mechanisms is how to make use of the laser ponderomotive force efficiently to pump a strong charge separation field in plasma, which is the origin of particle acceleration. Hence, it is the force (the accelerating force, the confining force, etc.) that people care about most in relativistic laser plasma physics. The effect of another important dynamical quantity, the torque, although as important as force, has not been revealed for a relativistic laser pulse. How to observe the orbital angular momentum (OAM) in laser-plasma interaction and how the appearance of OAM would essentially affect the process are of special interest. Circularly polarized light carries a spin angular momentum of $\pm\hbar$ per photon; however, the total OAM of a normal Gaussian pulse, commonly found in the current chirped pulse amplification technology, is zero. Therefore, observation of the torque and OAM in relativistic laser-plasma interaction is rare.

OAM has been discussed extensively for weak light [8–13] and extreme ultraviolet light [14–16]. Since Allen *et al.* first showed that a Laguerre-Gaussian (LG) laser pulse has finite OAM [8], many applications using twisted light have been found [9–11]. The OAM of a twisted light can be transferred to matter. More interestingly, several phenomena observed in astrophysics, like pulsars, are related to the OAM of light and plasma [17,18]. Thus, simulating and investigating such an immense process in a laboratory on the Earth would be of great convenience. Recently, Mendonca *et al.* have derived the solutions of plasma wave with OAM [19,20]. They also created a donut plasma wakefield using an intense laser with OAM for positron and electron acceleration [21,22]. Also an electron beam with OAM has drawn much interest [23,24], which may be derived from twist light interaction with plasma. However, as we know, an effective way to produce such an intense laser with OAM is still not provided.

Although several methods are available for obtaining twisted laser pulses, a relativistic twisted light pulse has not been generated yet. Since intense LG pulses are also useful elsewhere, there have been several attempts to produce them with the direct approach. However, because the amplified spontaneous emission in the middle of the laser pulse is inevitably very large during amplification, the amplified laser is no longer a LG pulse. The OAM effect of relativistic laser-plasma interaction remains unknown. In this Letter, we propose a simple and effective method for generating a relativistic twisted laser pulse and showing the OAM effect. It is called "light fan": a relativistic laser pulse (with a very high photon density) impinges on a spiral foil (the fan); hence, both the fan and the reflected pulse achieve a net large OAM. This study demonstrates that a reflect fan structure can be applicable in the relativistic regime. More importantly, the dynamic process of such a structure presents new and unique features in the relativistic intensity regime.

The proposed scheme is verified by the following three-dimensional (3D) particle-in-cell simulations. The setup is sketched in Fig. 1. The planar wave front of normal incident laser pulse in Fig. 1(a) is transformed to a helical wave front in Fig. 1(b) after the laser reflecting from the fan. In Fig. 1(c), the foil consists of eight parts with the same step height $\Delta h = \lambda/16$ to mimic a $\lambda/2$ spiral phase plate. If the foil acts as a perfect reflection mirror, the colors represent different phase changes when a plane wave is of normal incident. The maximum thickness of the foil is set as

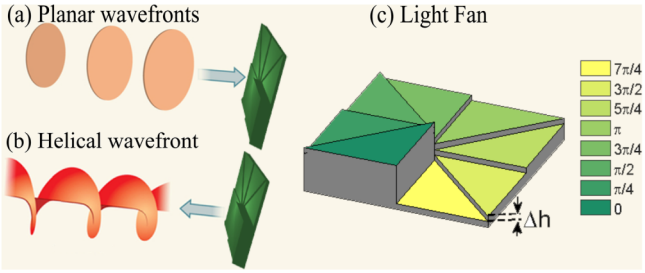

FIG. 1 (color online). (a) The normal incident laser pulse has a planar wave front. (b) The reflected laser pulse gets a helical wave front. (c) The foil used in the simulation has eight parts, with the same step height $\Delta h = \lambda/16$ to mimic a $h = \lambda/2$ spiral phase plate. The colors represent different phase changes when a plane wave incidents normally and the foil acts as a perfect reflection mirror. The maximum thickness of the foil is set as 0.8 μm to ensure that the laser pulse is not transmitted.

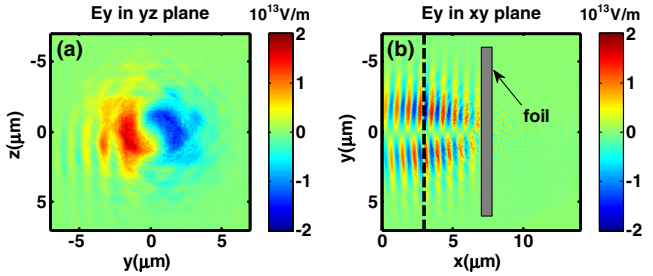

FIG. 2 (color online). Electric field E_y distribution in (a) the y-z plane of $x = 3.0$ μm and (b) the x-y plane of $z = 0.0$ μm at $t = 51.3$ fs when the beam is totally reflected. The black dashed line shows the x position of the plane in (a). An animation in the Supplemental Material [26] is provided by changing the x ($x = idx$) position of the plane in (a).

0.8 μm to ensure that the laser pulse is not transmitted. A relativistic laser pulse is of normal incident on the foil from the left, interacts with the matter, and is then reflected. The 0.8 μm laser pulse with the Gaussian time envelope $a(t) = a_0 \exp(-t^2/\Delta t^2)$ is linearly polarized along the y axis, and has a peak amplitude of $a_0 = 5$, pulse duration of $\Delta t = 13.3$ fs, and spot size of $w = 3\,\mu$m, where $a_0 = eE_y/m_e\omega_0 c$ is the normalized dimensionless laser electric field. The spiral foil has a density of $100n_c$, where $n_c = m_e\omega_0^2/4\pi e^2$ is the critical density. The simulation box is 15 μm $\times$ 20 μm $\times$ 20 μm in the $x \times y \times z$ directions, respectively. The foil is initially located between $x = 7.0$ μm and $x = 7.8$ μm. The simulation mesh size is $dx = 0.025$ μm in the x direction and $dy = dz = 0.05$ μm in the y and z directions. The number of macroparticles per cell is PPC = 2.

First, the distributions of E_y in the y-z plane of $x = 3.0$ μm [Fig. 2(a)] and the x-z plane of $z = 0.0$ μm [Fig. 2(b)] at time $t = 51.3$ fs when the beam is totally reflected are provided. This shows clearly the characters of twisted light. When the plasma surface is seen as a structured mirror, which is an approximate assumption in many cases, the reflected light mode can be expanded with a series of LG modes [25]. The amplitude LG_{nm} is defined by

$$\begin{aligned}\mathrm{LG}_{nm}(\rho,\phi,x) &= (C_{nm}/w)\exp(-ik\rho^2/2R)\exp(-\rho^2/w^2)\\ &\times \exp[-i(n+m+1)\psi]\\ &\times \exp[-i(n-m)\phi](-1)^{\min(n,m)}\\ &\times (\rho\sqrt{2}/w)^{|n-m|}L^{|n-m|}_{\min(n,m)}(2\rho^2/w^2), \qquad (1)\end{aligned}$$

with $R(x) = (x_R^2 + x^2)/x$, $\frac{1}{2}kw^2(x) = (x_R^2 + x^2)/x_R$, $\psi(x) = \arctan(x/x_R)$, where C_{nm} is a normalization constant, $k = 2\pi/\lambda$ is the wave number, x_R is the Rayleigh range, and $L_p^l(x)$is the generalized Laguerre polynomial. The Gaussian mode of the incident laser beam in the simulation is the LG_{00} mode. The mode decomposition of a LG_{00} mode whose wave front has been modified by the fan structure is then defined by the expansion coefficients [25]

$$\begin{aligned}a_{st} &= \langle \mathrm{LG}_{st}|\exp(-i\Delta\phi)|\mathrm{LG}_{00}\rangle\\ &= \iint \rho d\rho d\phi (C^*_{st}/w_{st})\exp(ik\rho^2/2R_{st} - \rho^2/w_{st}^2)\\ &\times \exp[-i(s-t)\phi](-1)^{\min(s,t)}(\rho\sqrt{2}/w_{st})^{|s-t|}L^{|s-t|}_{\min(s,t)}\\ &\times (2\rho^2/w_{st}^2)\exp(-i\Delta\phi)\\ &\times (C_{00}/w)\exp(-ik\rho^2/2R - \rho^2/w^2), \qquad (2)\end{aligned}$$

where

$$\Delta\phi = \sum_{n=0}^{7} H\left(\phi - \frac{\pi}{4}n\right)H\left(\frac{\pi}{4}n + \frac{\pi}{4} - \phi\right)\frac{2\pi}{8}n. \qquad (3)$$

$H(x)$ is the Heaviside function. Because of the fact that $\Delta\phi \approx \phi$, only the modes with $l = s - t = 1$ will contribute most in the ϕ integral. According to the animation [see Supplemental Material [26], distributions of E_y in the y-z plane changing with different x ($x = idx$) and laser wavelength corresponding to $\Delta i = \lambda/dx = 32$], the number of intertwined helices can be found to be $l = 1$. In the numerical calculation of Eq. (2), the Rayleigh range and the waist of the reflected light are assumed to be equal to those of the incident beam, respectively (i.e., $R_{st} = R$, $w_{st} = w$). The relative weight of the modes is given by $I_{st} = |a_{st}|^2$. Our calculations show that $I_{10} \approx 64.8\%$ and $I_{21} \approx 13.6\%$. We obtain a good approximation on the distributions of the reflected light electric field using $\sqrt{0.65}\mathrm{LG}_{10} + e^{i\theta}\sqrt{0.14}\mathrm{LG}_{21}$, where θ is the relative phase chosen to make the approximation closer to the simulation results (in our case, $\theta = \pi/2$).

In the theory of LG beam, the ratio of the angular momentum flux J to the energy flux P_L is $J/P_L = l/\omega$ [8]. According to the laser parameters in the simulations, the total OAM is about $L = lP_L\Delta t/\omega = 3.0 \times 10^{-17}$ kg m^2 s^{-1}, which agrees well with the OAM

sum of electrons and protons in scale and direction (Fig. 3). In addition, the total OAM of the reflected light is calculated based on the electromagnetic field data from the particle-in-cell simulations. The result is $\overrightarrow{L_x} = \varepsilon_0 \iint \vec{r} \times (\vec{E} \times \vec{B}) dt d\vec{r} = 1.1 \times 10^{-17}$ kg m^2 s^{-1}, which is close to the result of LG beam theory.

The statistical OAM in the x direction of the electrons and protons $L_x = \sum (\vec{r} \times \vec{p})_x$ at different times is given in Fig. 3(a). It shows that the OAM of both electrons and protons are oscillating with time, and that the frequency is the same as driven laser frequency. However, the proton OAM falls behind a phase π relative to electron OAM. The former obtains a net OAM $L_{px} = -2.0 \times 10^{-17}$ kg m^2 s^{-1} [blue circles in Fig. 3(a)] and the latter only oscillates around zero [red stars in Fig. 3(a)]. On the surface of the foil, any two opposite parts that are symmetric about the center will feel the laser field with a π phase difference, resulting in a significant OAM. As the laser field wave interacts with the foil, both electrons and protons rotate clockwise and anticlockwise under the action of the laser field and charge separation field. As we know, the angular momentum of a rotating disk is $L = 0.5\pi r^4 \rho h \omega$, where r is the radius of the disk, ρ the density, h the thickness, and ω the angular velocity. If we see the rotator as a proton disk with $r = 3$ μm, $h = 0.8$ μm, and $\rho = 100 m_p n_c$, the angular velocity corresponding to $L = 2.0 \times 10^{-17}$ kg m^2 s^{-1} is about $\omega = 7 \times 10^8$ rad s^{-1}. It can be one order higher than man-made rotational speed record 6×10^7 rad s^{-1}, which is also laser induced [16]. The rotation of the plasma after the laser pulse leaves may be used to simulate the pulsars [18].

Figure 3(b) (red pluses) shows the sum of the OAMs of electrons and protons $L_x = -2.0 \times 10^{-17}$ kg m^2 s^{-1}, which is the same with the calculated OAM of the reflected beam in scale and is the opposite in direction. The fitting curve of the total OAM [red dashed line in Fig. 3(b)] is based on the assumption that the torque $\tau_L = \partial L_x / \partial t$ changes with the longitudinal laser pulse envelope $\tau_L = 10^{-3} \exp\{-[(t - 37 \text{ fs})/13.3 \text{ fs}]^2\}$ N m [blue solid line in Fig. 3(b)], where 37 fs is the arrival time of the laser peak on the foil surface. The peak torque corresponds to the peak intensity of the laser, and the fastest variation of OAM. The head and tail of torque distribution corresponds to the head and tail of the laser pulse envelope, and the flat part of OAM. A torque of 10^{-3} N m can be given to a disk with a radius of about 3 μm by such a relativistic laser. It indicates that a huge OAM can be transported to a small volume in a very short time. The twisted light with the strongest torque by far can be found in twisted laser-driven HHG experiments. In the experiments of Zurch *et al.* [16], a 800 nm laser is reflected from the spatial light modulator to obtain a twisted light with peaking intensities of approximately 2×10^{15} W cm^{-2} focusing on a spot size of 40 μm. Assuming the best transformation (Gaussian mode totally converted to a series of LG modes with $l = 1$), the torque that such an intensity can provide to a 3 μm disk is about 8×10^{-8} N m. So the torque of relativistic twisted light in our plan can be 4 orders higher. In our case, the OAM density of relativistic twisted light, defined with OAM over volume, can be as high as $u = L_x/V = 0.56$ kg m^{-1} s^{-1}. Considering that high energy density is an important concept, this high OAM density may bring some new effects. Similar to the ponderomotive force originating from the inhomogeneity of laser intensity, the torque comes from both the laser intensity distribution and helical phase fronts. The torque is an intrinsic characteristic like the ponderomotive force. Thus, we should expect that the torque characteristic will be as important as the ponderomotive force in relativistic light-matter interaction, and brings out some potential applications.

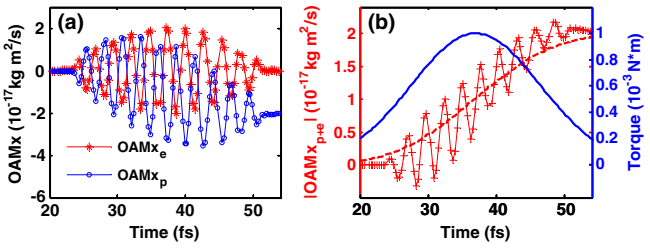

FIG. 3 (color online). (a) OAM (in the x direction) of electrons (red stars) and protons (blue circles) changing with time. (b) Sum of the OAMs of electrons and protons (red plusses) changing with time; the blue solid line is fitted based on the assumption that the torque changes with the longitudinal laser pulse envelope $\tau_L = 10^{-3} \exp\{-[(t - 37 \text{ fs})/13.3 \text{ fs}]^2\}$ N m. Integration of the torque gives the fitting OAM curve (red dashed).

Figure 4 shows the changes of the total OAM when keeping the power unchanged for different spot sizes. The results of the two different powers, $P_0 = 4.8 \times 10^{12}$ W (blue squares) and $P_1 = 4.3 \times 10^{13}$ W (red circles), are shown. The total OAM almost also keeps unchanged for a constant power. It can be easily understood from the view of OAM conservation between light and plasma. For the light, the ratio of the angular momentum flux to the energy flux is decided only by the number of intertwined helices [8], then the total step height. So the same power brings the same OAM, and the higher power brings the higher OAM. The small decrease of OAM when spot size reduces can be

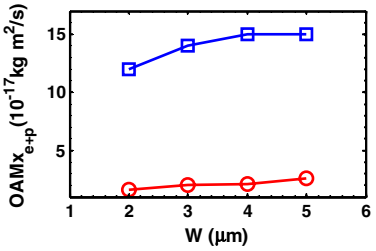

FIG. 4 (color online). The effect of laser spot size. The results of the two different powers, $P_0 = 4.8 \times 10^{12}$ W (blue squares) and $P_1 = 4.3 \times 10^{13}$ W (red circles), corresponding to $a_0 = 5$ and $a_1 = 15$, respectively, when the spot size is 3 μm.

understood as follows. With a smaller spot size and a higher intensity, the structure of foil may deform more heavily in the later process of laser-plasma interaction. Given the deviation from the spiral step structure, the total OAM of matter or light decreases slightly. Based on theory of LG, the peak OAM density of the LG beam is $u = lI_0/(c\omega)$, where I_0 is the peak laser intensity. Then the OAM density of the relativistic twisted beam can be very huge due to the high intensity of the relativistic beam. It also shows that the OAM density can be higher when the laser beam focuses smaller. In experiments, the precision of the focal region on the target is a common problem. We did some simulations for the case of deviations. It was found that the characteristics of twist light and the related OAM effects were still clear when deviations did not exceed a tolerance (not shown). A theoretical calculation of the relative weight of LG_{10} shows that a larger laser spot size results in a larger tolerance.

Up to now, OAM is emphasized only in conventional optics. Apart from the phase change carried out in optics, this work reveals the dynamic process of relativistic laser interaction with plasma, which has not been completely elucidated. Combined with other schemes of relativistic mirrors in plasma (ion acceleration, coherent radiation with high energy, hot electron transport) [27], OAM in the relativistic light-matter interaction may bring new effects. For example, the relativistic attosecond x-ray vortices from HHG should also be expected. Consequential explorations about the effects of OAM on various aspects, such as transport of hot electrons, proton acceleration, and plasma wave, may become available. Using relativistic tabletop lasers, this scheme creates a new laboratory plasma regime with extreme plasma parameters, such as huge OAM. It may be used to mimic some astrophysical environments such as the pulsars [18].

As an important characteristic, the relativistic laser has a strong torque. This strong torque can lead to a strong OAM when the laser interacts with structured matter (such as the light fan in our case) or when twisted light (such as the reflected light in our case) interacts with uniform matter. Just as the strong ponderomotive force of a relativistic laser can produce a finite linear momentum in many applications (for example, laser wakefield acceleration), such a strong torque should also be expected to produce a finite OAM in many potential applications. Also, a relativistic twisted laser has an ultrahigh OAM density accompanying ultrahigh energy density. We expect experiments based on the light-fan scheme can be realized soon, which should lead to some novel results on strong laser field physics [28].

This work was supported by the Ministry of Science and Technology (Grants No. 2011DFA11300, No. 2011CB808104), and the National Natural Science Foundation of China (Grants No. 61221064, No. 11125526, No. 11335013, No. 11127901).

*To whom all correspondence should be addressed.bfshen@mail.shcnc.ac.cn

[1] G. A. Mourou, T. Tajima, and S. V. Bulanov, Rev. Mod. Phys. **78**, 309 (2006).
[2] E. Esarey, C. B. Schroeder, and W. P. Leemans, Rev. Mod. Phys. **81**, 1229 (2009).
[3] A. Macchi, M. Borghesi, and M. Passoni, Rev. Mod. Phys. **85**, 751 (2013).
[4] U. Teubner and P. Gibbon, Rev. Mod. Phys. **81**, 445 (2009).
[5] S. Corde, K. Ta Phuoc, G. Lambert, R. Fitour, V. Malka, A. Rousse, A. Beck, and E. Lefebvre, Rev. Mod. Phys. **85**, 1 (2013).
[6] E. N. Nerush, I. Y. Kostyukov, L. Ji, and A. Pukhov, Phys. Plasmas **21**, 013109 (2014).
[7] L. L. Ji, A. Pukhov, E. N. Nerush, I. Y. Kostyukov, B. F. Shen, and K. U. Akli, Phys. Plasmas **21**, 023109 (2014).
[8] L. Allen, M. W. Beijersbergen, R. J. C. Spreeuw, and J. P. Woerdman, Phys. Rev. A **45**, 8185 (1992).
[9] D. G. Grier, Nature (London) **424**, 810 (2003).
[10] G. Molina-Terriza, J. P. Torres, and L. Torner, Nat. Phys. **3**, 305 (2007).
[11] A. M. Yao and M. J. Padgett, Adv. Opt. Photonics **3**, 161 (2011).
[12] L. Shi, L. Tian, and X. Chen, Chin. Optic. Lett. **10**, 120501 (2012).
[13] M. Kang, Y. Yao, K. Xia, Z. Fang, and J. Li, Chin. Optic. Lett. **11**, 051401 (2013).
[14] C. Hernández-García, A. Picón, J. San Román, and L. Plaja, Phys. Rev. Lett. **111**, 083602 (2013).
[15] E. Hemsing, A. Knyazik, M. Dunning, D. Xiang, A. Marinelli, C. Hast, and J. B. Rosenzweig, Nat. Phys. **9**, 549 (2013).
[16] M. Zurch, C. Kern, P. Hansinger, A. Dreischuh, and C. Spielmann, Nat. Phys. **8**, 743 (2012).
[17] H. Martin, Astrophys. J. **597**, 1266 (2003).
[18] S. V. Bulanov, T. Z. Esirkepov, D. Habs, F. Pegoraro, and T. Tajima, Eur. Phys. J. D **55**, 483 (2009).
[19] J. T. Mendonça, B. Thidé, and H. Then, Phys. Rev. Lett. **102**, 185005 (2009).
[20] J. T. Mendonca, S. Ali, and B. Thidé, Phys. Plasmas **16**, 112103 (2009).
[21] J. T. Mendonça and J. Vieira, Phys. Plasmas **21**, 033107 (2014).
[22] J. Vieira, and J. T. Mendonça, Phys. Rev. Lett. **112**, 215001 (2014).
[23] K. Y. Bliokh, Y. P. Bliokh, S. Savel'ev, and F. Nori, Phys. Rev. Lett. **99**, 190404 (2007).
[24] B. J. McMorran, A. Agrawal, I. M. Anderson, A. A. Herzing, H. J. Lezec, J. J. McClelland, and J. Unguris, Science **331**, 192 (2011).
[25] M. W. Beijersbergen, R. P. C. Coerwinkel, M. Kristensen, and J. P. Woerdman, Opt. Commun. **112**, 321 (1994).
[26] See Supplemental Material at http://link.aps.org/supplemental/10.1103/PhysRevLett.112.235001 for distributions of E_y in the $y-z$ plane changing with different x.
[27] S. V. Bulanov, T. Z. Esirkepov, M. Kando, A. S. Pirozhkov, and N. N. Rosanov, Phys. Usp. **56**, 429 (2013).
[28] T. Brabec, *Strong Field Laser Physics* (Springer, New York, 2008).